J Incl Phenom Macrocycl Chem (2010) 66:231–241
DOI 10.1007/s10847-009-9615-9

ORIGINAL ARTICLE

Inclusion complexes of cationic xanthene dyes in cucurbit[7]uril

Ronald L. Halterman · Jason L. Moore · Krystle A. Yakshe · Julie A. I. Halterman · Kevin A. Woodson

Received: 10 March 2009 / Accepted: 9 June 2009 / Published online: 28 June 2009

Abstract Improvements in optical properties of organic xanthene fluorophores through molecular encapsulation in cucurbit[7]uril (CB7) should enable better molecular probes and devices to be designed. Although the interactions of several dyes with CB7 have been studied, the data have often been incomplete. Uniformly applied ensemble spectroscopic studies are presented herein, including ^{1}H NMR, UV–Vis, and fluorescence titration experiments of aqueous CB7 complexes with the monocationic xanthene dyes rhodamine 6G (Rh6G, **1**), rhodamine B (RhB, **2**), rhodamine B benzyl ester (RhBBE, **3**), pyronin B (PyB, **4**) and pyronin Y (PyY, **5**). All of these cationic xanthene dyes formed 1:1 complexes with cucurbit[7]uril as evidenced by NMR data and Job's plots of fluorescence changes upon addition of CB7. Non-linear regression analysis of the fluorescence titration curves gave precise K_a's for RhB, RhBBE and PyB between 1.1×10^5 M^{-1} and 9.1×10^6 M^{-1}. The fluorescence emission intensity of Rh6G was lowered 0.8-fold in the presence of CB7 while the other dyes examined showed an increase between 1.3 and 4.7-fold. NMR titration experiments from 0 to 2.0 equivalents of CB7 per equivalent of xanthene gave in only some cases very clear evidence of inclusion complexation. Non-specific adsorption of these xanthene dyes onto borosilicate glass was very pronounced and could be inhibited by dye inclusion into CB7.

Keywords Cucurbit[7]uril · CB7 · Rhodamine · Pyronin · Inclusion complex

Introduction

In recent years much organic dye research has focused on the development of technologies such as molecular scale biological probes and sensors [1–7]. However, the use of organic dyes for these types of applications has been slowed due to several limitations including undesirable aggregation, fluorescence blinking and photobleaching, surface adsorption and relatively poor photostability [8–15]. These problems can in principle be reduced by supramolecular encapsulation, especially in terms of minimizing aggregation and surface adsorption [8, 16, 17]. While the bulk of this type of research has been performed using β-cyclodextrin as a host, recent efforts have started to examine the effect of cucurbit[7]uril (abbreviated as CB7 or Q7) [18–21] on the photophysical and photochemical behavior of fluorophores and in particular common fluorescent dyes [9, 15, 22–28]. Results by Nau and co-workers have shown that the addition of cucurbit[7]uril to aqueous solutions of rhodamine 6G resulted in several advantageous effects including enhanced brightness and fluorescence lifetimes and a reduction of non-specific adsorption and aggregation [16, 29]. In order to better understand these effects as they relate to cationic organic dyes of interest, we present here ensemble spectroscopy studies, including ^{1}H NMR, UV–Vis, and fluorescence titration experiments of cucurbit[7]uril complexes with the monocationic xanthene dyes rhodamine 6G (Rh6G, **1**), rhodamine B (RhB, **2**), rhodamine B benzyl ester (RhBBE, **3**), pyronin B (PyB, **4**) and pyronin Y (PyY, **5**). The formula structures of these compounds are shown in Fig. 1.

Electronic supplementary material The online version of this article (doi:10.1007/s10847-009-9615-9) contains supplementary material, which is available to authorized users.

R. L. Halterman (✉) · J. L. Moore · K. A. Yakshe · J. A. I. Halterman · K. A. Woodson
Department of Chemistry and Biochemistry, University of Oklahoma, 620 Parrington Oval, Norman, OK 73019, USA
e-mail: rhalterman@ou.edu

The widely studied fluorescent dye rhodamine 6G was investigated to provide calibration between our work and literature reports on some of the properties of rhodamine 6G—cucurbit[7]uril mixtures [15, 16]. Related confocal microscopy studies on the fluorescence of single molecules of rhodamine 6G in CB7 films have also been reported by our research group [30]. The other xanthene dyes were studied to probe the changes in binding and photophysical properties in response to structural changes on the xanthene core. For each of the dyes, we performed NMR, absorption and fluorescence titration experiments, as well as Job's plot and linear regression analyses to characterize the binding and photophysical properties of the complexes with CB7. As detailed herein we did find that xanthenes without the 9-aryl substituent generally gave stronger binding to CB7. Greater perturbations in the chemical shifts in NMR spectra and smoother fluorescent titration curves were seen with the xanthenes containing *N,N*-diethylamino groups.

Results and discussion

Rhodamine 6G (Rh6G, **1**)

Some steady state and time resolved photophysical properties of aqueous rhodamine 6G in the presence of CB7 have been reported, usually as summaries of unpublished raw data [15, 16]. Enhanced absorbance and fluorescence lifetimes and intensity in the presence of CB7 were observed and NMR titration data and Job's plots were cited as being consistent with a 1:1 binding model of the dye and CB7 [15]. Although it is apparent that CB7 interacts with Rh6G to decrease surface adsorption and to improve the photophysical properties, the nature of that interaction has not been conclusively made. In order to establish a solid basis for comparisons between the dye–CB7 complexes, we remeasured some of these reported properties and the data we provide have some differences from the data summarized in the literature. The absorbance and fluorescence emission spectra for aqueous 2.5 μM rhodamine 6G prepared in polystyrene cuvettes without and in the presence of 1 mM CB7 are shown in Fig. 2.

Essentially no shift in the wavelength and a modest *decrease* in the absorbance (0.9-fold) and fluorescence intensity (0.8-fold) were noted in the presence of CB7. A change in the absorbance shoulder near 490 nm could indicate a change in dye–dye aggregation [31]. For this dye and the other cationic xanthene dyes in this study we found it difficult to use the absorbance data to generate titration curves. Changes in the known H- and J-type aggregation upon CB7 complexation often led to significant changes in the absorbance spectra. Since the absorbance changes often decreased then increased with increasing CB7 concentration, we chose the smoother changes obtained in the fluorescence spectra for our CB7 titration curves. The complete titration spectra are provided in the supplementary data (Fig. S3). In contrast, Nau reported a modest increase in both the absorbance and fluorescence intensity upon

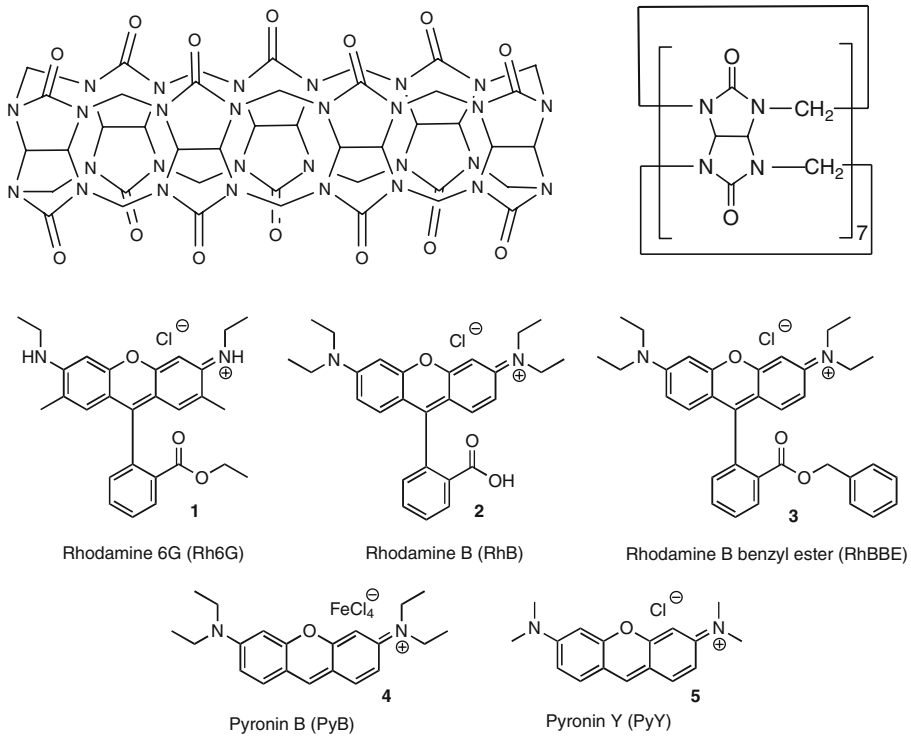

Fig. 1 Structures of CB[7] and xanthene dyes used in this study

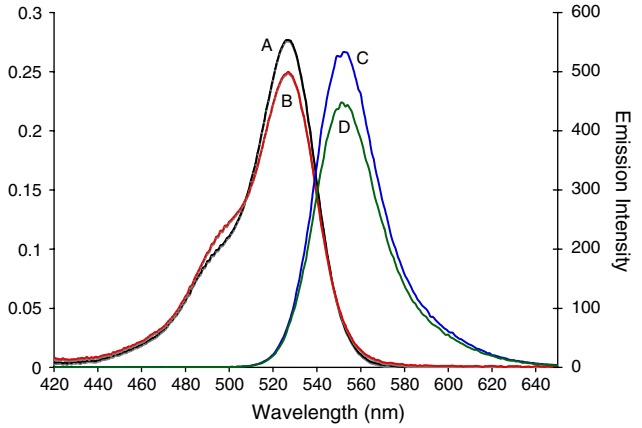

Fig. 2 UV–VIS absorption spectra (**a** at 0 mM CB7 and **b** at 1 mM CB7) and fluorescence emission spectra (**c** at 0 mM CB7 and **d** at 1 mM CB7) of aqueous rhodamine 6G (2.5 μM) in polystyrene cuvettes

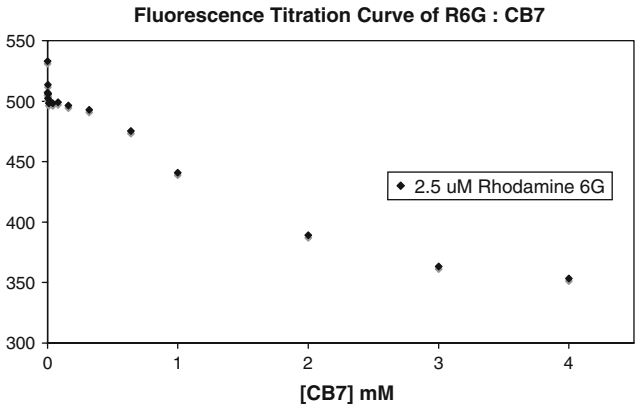

Fig. 3 Titration curve of fluorescence emission signal intensity of aqueous rhodamine 6G (2.5 μM) and CB7 (0–4 mM) prepared in polystyrene cuvettes upon excitation at 527 nm

addition of a 1 mM solution of CB7 to a 1 μM solution of Rh6G [15]. When we prepared aqueous samples of 3 μM Rh6G without and in the presence of up to 4 mM CB7 in borosilicate glass vials and sequentially transferred the samples to a quartz cuvette for each absorbance and then fluorescence measurement, we also observed a 2.1-fold *increase* in absorbance and a 2.5-fold increase in fluorescence intensity in the presence of CB7 (Figs. S4 and S5). Given Nau's solid evidence for non-specific adsorption of Rh6G onto borosilicate glass [15, 16], the enhancement factors we observed under these conditions were less likely to be primarily due to a photophysical enhancement but rather due to differential non-specific adsorption of the Rh6G onto the walls of the vials during the 1-2 h between sample preparation and completing the spectroscopic measurements. When insufficient CB7 was present the Rh6G non-specifically adsorbed to the borosilicate glass. When the solution was transferred to a cuvette for optical measurements, a lower concentration of total dye (bound to CB7 and free) was present. When a sufficient amount of CB7 was present the dye–CB7 complex remained in solution at maximum concentration.

The titration curve for changes in fluorescence intensity of 2.5 μM R6G and 0 to 4 mM CB7 prepared in polystyrene cuvettes (Fig. 3) appears to indicate an initial 1:1 binding with saturation occurring at less than 0.1 mM CB7. However, the fluorescence intensity then continues to vary as the CB7 concentration is increased up to 4 mM. A non-linear regression analysis of the low CB7 concentration data up to 0.1 mM gave a tentative 1:1 binding constant of $1.2 \pm 0.4 \times 10^6\ M^{-1}$, a value which is fraught with potential error since no data was included for CB7 at higher concentrations where what could be an inflection point near 0.2 mM CB7 was seen (Figs. S7 and S8). Analyses using the full data set up to 4 mM CB7 failed to give a valid binding constant. Although the continuous variation Job's plot of absorbance provided in Fig. S6 was most consistent with a strong 1:1 binding of rhodamine 6G and CB7 [32, 33], a shoulder in the Job's plot curve between 0.5 and 0.6 could be due to subsequent, weaker interactions at higher CB7 concentrations. The nature of the additional interactions between Rh6G and CB7 could not be extracted from the data.

The fluorescence titration curve of aqueous Rh6G (3 μM) prepared in borosilicate glass is shown in Fig. 4. Rather than showing a *decrease* in signal intensity as was observed for samples prepared in polystyrene cuvettes, this series shows an initial *increase* in signal intensity, followed by a small decrease in signal strength at higher concentrations of CB7. In this borosilicate glass case, the increase in signal intensity was likely due to decreasing the amount of non-specific adsorption of Rh6G as the CB7 concentration increased and a corresponding increase in the concentration of total dye in solution. With no CB7 present much of the Rh6G could adsorb onto the borosilicate glass, reducing the dye concentration in solution. Samples containing

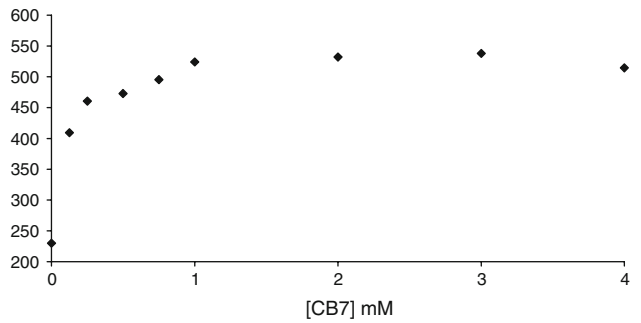

Fig. 4 Fluorescence emission titration curve of aqueous rhodamine 6G (3 μM) and CB7 (0–4 mM). Samples were prepared in borosilicate glass vials and the fluorescence emission spectra were obtained in quartz cuvettes

increasing amounts of CB7 resulted in increased amounts of dye–CB7 complex in solution and a higher total dye concentration. Once enough CB7 was present to minimize non-specific binding of the Rh6G to the glass surface, the gradual decrease in signal strength was similar to the samples prepared in polystyrene. An initial binding value can be calculated for the increase in signal strength (1×10^4 M^{-1}) due primarily to increased total dye concentration as a result of decreased non-specific adsorption. This binding value approached that obtained for the R6G-CB7 titration in polystyrene. Titration curves in both polystyrene and borosilicate glass were essentially measuring parallel effects of the same CB7 binding—either photophysical changes upon binding and/or protection from non-specific adsorption. The similarity of these outcomes could easily lead to misinterpretation of titration data.

NMR titration experiments resulted in only minor perturbations in the spectra of aqueous rhodamine 6G as CB7 was added (Fig. S9). At the high 4.2 mM concentration of Rh6G, changes in non-specific binding with increasing CB7 concentration were unlikely to be as significant as at the micromolar concentrations used for the optical measurements. In stable inclusion complexes, signals for hydrogen atoms well inside the CB7 cavity are usually strongly shifted to higher field, while those near the carbonyl portals show little perturbation or a downfield shift [27, 28, 34]. While the photophysical and stability properties indicate binding and probably inclusion of rhodamine 6G into CB7, the NMR spectra did not exhibit the expected strong shifts for a stable inclusion complex having hydrogen atoms well within the CB7 cavity. Based on molecular models it is likely that the 9-aryl group prevented the cationic xanthene core from inserting deeply into the CB7 cavity, leaving even the included portions of the guest near the CB7 portal. Furthermore, since only one set of signals was present throughout the NMR titration, an exchange of CB7 from one end of the xanthene core to the other could be likely and would average out and further minimize any chemical shift changes. Alternatively, the interaction may be a symmetric exclusion complex having the xanthene dye lying across the portal of the CB7. Given the importance of Rh6G as a laser dye and the established benefits upon adding CB7 to aqueous Rh6G [16], it was disappointing that a clearer binding model was not supported by our data.

Rhodamine B (RhB, **2**)

Rhodamine B is a commercially available, widely studied dye [10, 31, 35, 36] that structurally differs from rhodamine 6G in three ways: its xanthene core lacks the 2,7-dimethyl groups, it contains a 2-carboxylic acid group on the 9-phenyl moiety in place of the 2-ethoxycarbonyl group and it contains 3,6-bis(*N,N*-diethylamino) groups in place of the *N*-ethylamino groups. These structural changes were reflected in the binding and photophysical properties of rhodamine B with CB7.

The absorbance and fluorescence emission spectra for aqueous rhodamine B without and in the presence of CB7 were measured on samples directly prepared in polystyrene cuvettes. A modest 1.3-fold increase in absorbance as a function of an increase in the molar absorption coefficient (ε) from 8.0×10^4 M^{-1} cm^{-1} to 1.0×10^5 M^{-1} cm^{-1}, a slight bathochromic shift from 575 nm to 582 nm and a 1.6-fold increase in fluorescence intensity were noted upon addition of CB7. A symmetric Job's plot supports the formation of a 1:1 rhodamine B and CB7 complex (Fig. S11). The complete titration spectra are provided in Fig. S10 and a non-linear regression analysis of the fluorescence data gave a 1:1 binding constant of $1.6 \pm 0.4 \times 10^5$ M^{-1} (Figs. S12 and S13).

The ^{1}H NMR titration spectra in which the concentration of cucurbit[7]uril was varied and the concentration of rhodamine B was held constant are provided in Fig. 5. Unlike rhodamine 6G, there were very significant changes in the signals of both the xanthene hydrogens and the *N,N*-diethyl groups of rhodamine B upon addition of cucurbit[7]uril. Most noticeably, there was a broadening and an upfield shift of both the methylene and methyl signals of the *N,N*-diethyl hydrogens. It is most informative to follow the changes in the methyl signals. At the 1:1 and 1.5:1 ratios of CB7 to rhodamine B, the methyl signal was split into a broad pair of signals as would be consistent with a 1:1 complex between rhodamine B and cucurbit[7]uril in which the *N,N*-diethylamino groups were only slowly exchanging between included and free chemical environments. If the exchange between free and complexed methyl groups were fast, then a sharper averaged methyl signal would be expected. At the 1:1 ratio a new signal for what is likely an included methyl group was growing in near 0.7 ppm. When 1.5 equivalents of CB7 were present broadened signals for both bound (0.7 ppm) and free (1.2 ppm) methyl signals were observed. The exchange between free and bound was slow enough for these two signals to be observed separately. At 0.5 equivalents of CB7 the methyl signal was only broadened through what was likely an intermediate exchange process. If a stable, slowly exchanging 1:1 or even 2:1 RhB–CB7 complex were formed, then two sets of methyl signals would be expected (for free and bound methyls). At 2 equivalents of CB7, a single set of broad signals was observed as expected for intermediately exchanging sites. If a stable 1:2 RhB–CB7 complex were present, both methyl groups should be included and appear as a single sharp signal (likely near 0.7 ppm). Since the single signal near 0.9 ppm was broadened, some intermediate exchange between bound

and free methyl groups was likely taking place. These results support an associative exchange mechanism in which a second CB7 binds the non-included end of the xanthene core, but as the 2:1 complex is apparently not stable, the initial CB7 could depart as shown in Fig. 6.

The binding constant for rhodamine B is lower than the tentative one found for rhodamine 6G. Apparently any advantages that rhodamine B may have had through the thinner xanthene core without the 2,7-dimethyl groups or through the additional hydrophobic alkyl substitution on the 1,6-amino groups were outweighed by the advantages of the potential hydrogen bond donor on the *N*-ethylamino groups or the additional hydrophobic 2,7-dimethyl groups. The effect of having a 2-carboxylic acid or 2-carboxylic acid ester on the 9-aryl group will be discussed below. In the NMR spectra, however, the presence of the *N,N*-diethylamino groups on rhodamine B did lead to splitting of the ethyl signals into what are likely included and free environments.

Rhodamine B Benzyl Ester (RhBBE, **3**)

In order to more directly probe a potential factor for CB7-rhodamine binding strength, we converted the 2-carboxylic acid group on the 9-phenyl substituent of rhodamine B (**2**) into an ester. Benzyl ester **3** was readily prepared by a DCC-promoted coupling reaction [37] as shown in Scheme 1 and separated from unreacted rhodamine B through column

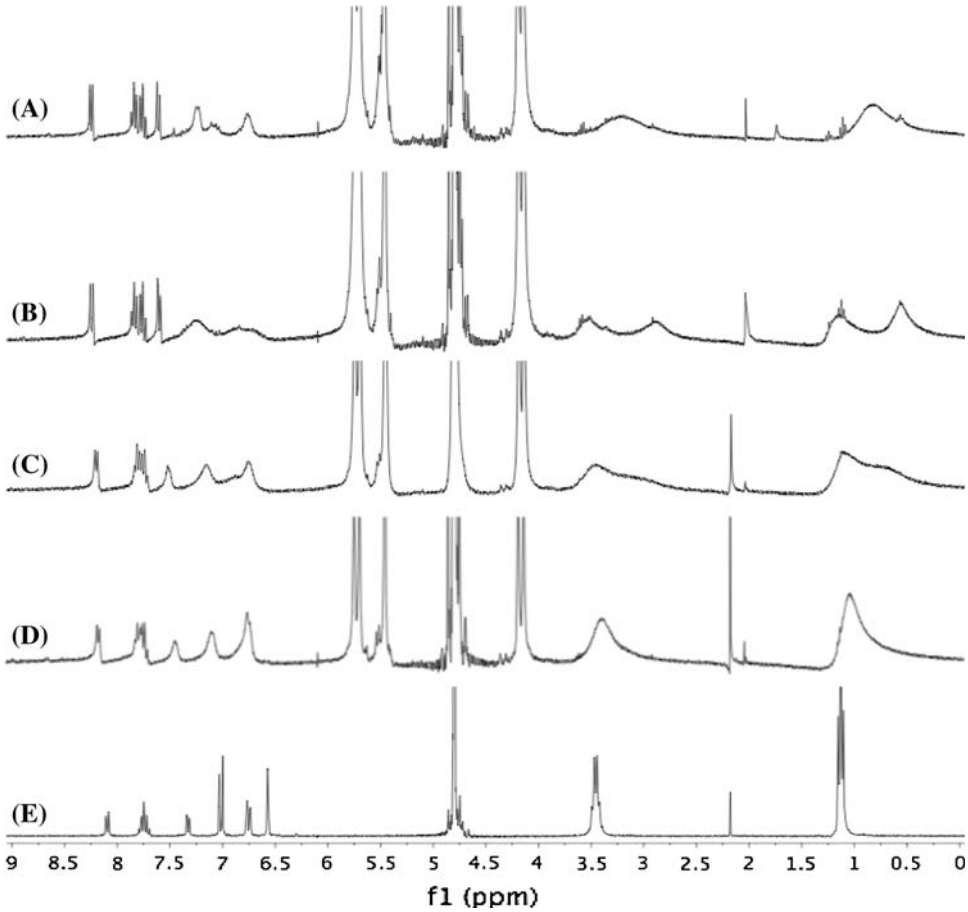

Fig. 5 ^{1}H NMR spectra (300 MHz, D_2O) of aqueous rhodamine B (4.2 mM) in the presence of 2.0 equivalent (**a**), 1.5 equivalent (**b**), 1.0 equivalent (**c**), 0.5 equivalent (**d**) and the absence (**e**) of CB7 (0–8.4 mM)

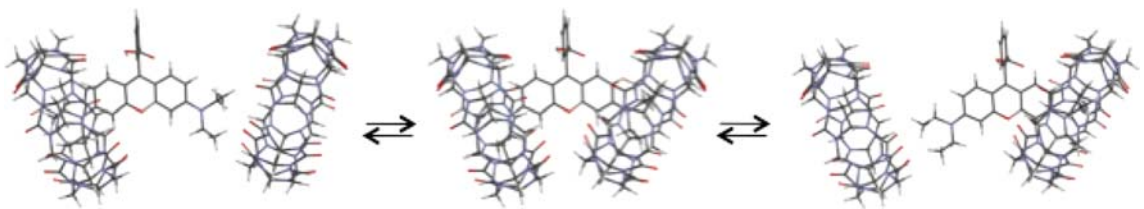

Fig. 6 Associative exchange of CB7 binding site on PyB

Scheme 1

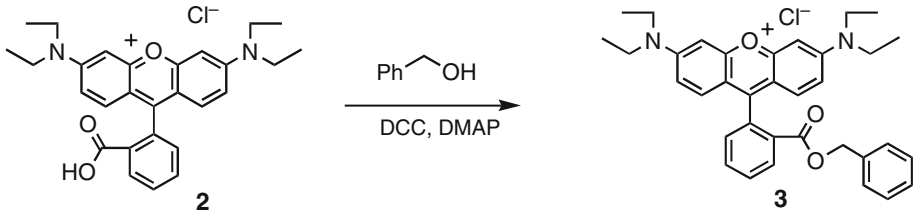

chromatography (SiO_2, 9:1 methanol/chloroform to elute unreacted RhB followed by 90:10:1 methanol/chloroform/glacial acetic acid to elute RhBBE) [31].

The absorbance and fluorescence emission spectra for aqueous rhodamine B benzyl ester (**3**) without and in the presence of CB7 were measured on samples prepared directly in polystyrene cuvettes and are shown in Fig. 7. A modest 1.6-fold increase in the absorbance as a function of an increase in the molar absorption coefficient (ε) from 2.4×10^4 M^{-1} cm^{-1} and 3.8×10^4 M^{-1} cm^{-1} upon addition of cucurbit[7]uril. In contrast to rhodamine B, a very sizable 4.7-fold increase in fluorescence intensity was noted upon addition of CB7 to the benzyl ester **3**. A symmetric Job's plot supports the formation of a 1:1 rhodamine B benzyl ester and CB7 complex (Fig. S15). The complete titration spectra are provided in Fig. S14 and a non-linear regression analysis gave a 1:1 binding constant of $1.1 \pm 0.16 \times 10^5$ M^{-1} (Figs. S16 and S17). The binding constant for rhodamine B benzyl ester was found to be lower than for rhodamine B by a 5-fold factor, indicating that the hydrogen bonding carboxylic acid group on the 9-aryl ring was more beneficial to binding than ester groups.

The ^{1}H NMR titration spectra in which the concentration of CB7 was varied from 0 to 2 equivalents per molecule of rhodamine B benzyl ester (3.5 mM) are provided in Fig. S18. Consistent with the formation of an inclusion complex, broadening of the *N,N*-diethylamino and xanthenyl hydrogen signals was observed. In contrast to the splitting seen for the *N,N*-diethylamino groups in the more strongly binding rhodamine B, the lower binding constant between rhodamine B benzyl ester and CB7 appeared to allow faster exchange and only gave averaged *N,N*-diethylamino signals.

Pyronin B (PyB, **4**)

Pyronin B is a flat cationic dye chosen for investigation due to its anticipated ability to be more completely encapsulated by cucurbit[7]uril [15]. It contains the same 3,6-bis(*N,N*-diethylamino) groups as rhodamine B, but lacks the 9-aryl substituent. Some photophysical properties of CB7 complexes of PyB and the 3,6-bis(*N,N*-dimethylamino) derivative PyY (**5**) have been reported by Nau, although the binding constants were not reported [15]. Absorbance and fluorescence emission spectra of aqueous PyB (2.5 μM) in the absence and presence of 0.64 mM CB7 were measured on samples directly prepared in polystyrene cuvettes and are shown in Fig. 8. No shift in the absorbance wavelength maximum (553 nm) for PyB was observed in the presence of cucurbit[7]uril. Essentially no change in the absorbance was observed at 0.64 mM CB7. In the fluorescence emission spectra a slight bathochromic shift in the fluorescence emission maximum from 569 nm to 570 nm for PyB and

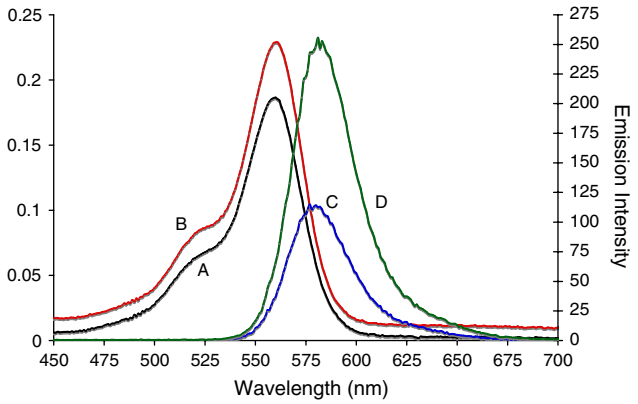

Fig. 7 UV–VIS absorption spectra (**a** at 0 mM CB7 and **b** at 0.64 mM CB7) and fluorescence emission spectra (**c** at 0 mM CB7 and **d** at 0.64 mM CB7) of aqueous rhodamine B benzyl ester (2.5 μM) in polystyrene cuvettes

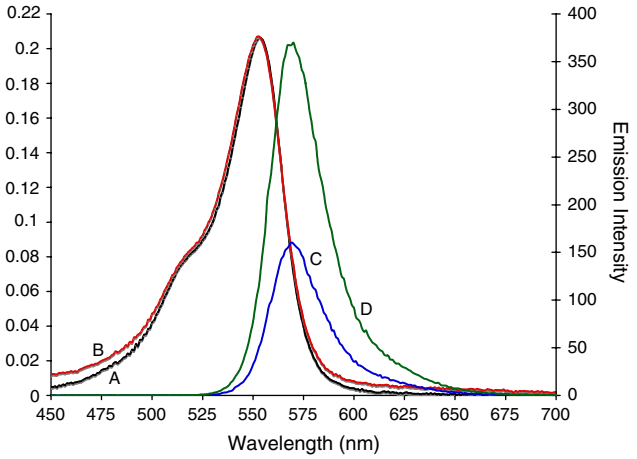

Fig. 8 UV–VIS absorption spectra (**a** at 0 mM CB7 and **b** at 0.64 mM CB7) and fluorescence emission spectra (**c** at 0 mM CB7 and **d** at 0.64 mM CB7) of aqueous pyronin B (2.5 μM). Samples prepared and spectra obtained in polystyrene cuvettes

2.3-fold increase in the fluorescence emission intensity were observed in the presence of 1.0 mM cucurbit[7]uril. A Job's plot of PyB and CB7 indicated the formation of a 1:1 complex (Fig. S20). Full titration plots for the absorbance and fluorescence emission spectra of PyB with increasing CB7 concentration are also given in Fig. S19. A non-linear regression analysis of the fluorescence titration gave a 1:1 binding constant of $9.1 \pm 1.6 \times 10^6\ M^{-1}$ (Figs. S21 and S22). The binding constant for pyronin B-CB7 was found to be significantly higher than for rhodamine B, indicating that the 9-aryl substituent appears to be detrimental to stronger binding.

The NMR titration spectra are shown in Fig. 9. As was seen for rhodamine B, the *N,N*-diethylamino groups gave a splitting of both the methylene and methyl groups at a 1:1 CB7:PyY ratio. We also observed a downfield shift of H-9 and H-1/H-8 on the xanthene core. The hydrogens adjacent to the amino group were strongly broadened and split into two sets of signals at the 1:1 ratio. At one equivalent of CB7 two signals for the methyl groups were clearly located near 0.7 ppm (bound) and 1.2 ppm (free) which indicates slow exchange of CB7 from one end of the PyB group to the other end. The onset of coalescence was likely at 1.5 equivalents of CB7. At 2.0 equivalents of CB7 a single but quite broad methyl signal was observed, indicating an intermediate exchange of CB7 from one end of PyB to the other end as was the case with the RhB sample. The increasing concentration of CB7 could facilitate the increase in exchange rate from slow to intermediate. The broad nature of the signals do not support a single stable 1:2 PyB–CB7 complex since such a complex should have given a sharper set of equivalent signals. These shifts and the sharpness of the more central hydrogen atoms are consistent with a partial insertion of PyY into the CB7 pocket as shown for the two minimized structures in Fig. 10. Semiempirical (PM3) calculations gave two lower energy gas phase structures with an energy difference of only 0.4 kcal/mol and aid us in visualizing favored structures that could contribute to a solution structure of the complex. The two broad sets of signals for the *N,N*-diethylamino groups indicate a slow exchange of the CB7 from one amino end of the xanthene to the other end. When a second equivalent of CB7 is present, the exchange is faster and a single set of broadened signals are observed. Even in the presence of excess CB7 the data do not fit a stable 2:1 binding of CB7 and PyY since broadened signals are present rather than the sharp signals expected for a stable symmetric complex.

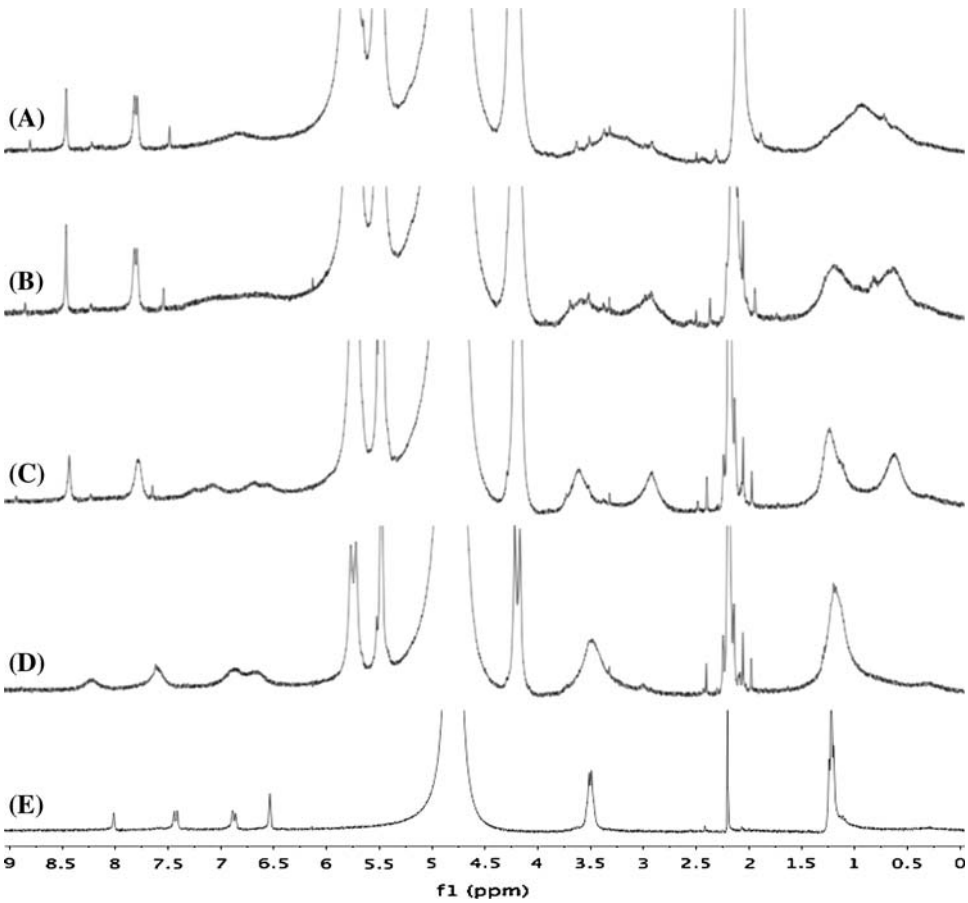

Fig. 9 ^{1}H NMR spectra (300 MHz, D_2O) of pyronin B in the presence of 2.0 equivalent (**a**), 1.5 equivalent (**b**), 1.0 equivalent (**c**), 0.5 equivalent (**d**) and the absence (**e**) of CB7

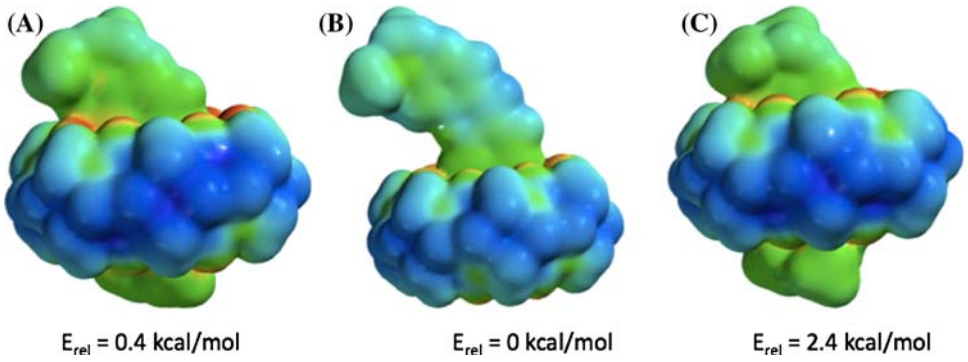

Fig. 10 PM3-calculated (Wavefunction MacSpartan program) gas-phase structures of PyB-CB7. **a** and **b** Lower energy with PyB non-symmetrically inserted in CB7. **c** Higher energy with PyB centered in CB7

Pyronin Y (PyY, **5**)

Pyronin Y is a flat cationic dye chosen for investigation due to its anticipated ability to be more completely encapsulated by cucurbit[7]uril and to provide comparison data on the effects of *N,N*-diethylamino versus *N,N*-dimethylamino groups on the binding of cationic xanthene dyes to CB7. As was initially done with Rh6G, dilute solutions of PyY were prepared in borosilicate glass vials which were then sequentially transferred to quartz cuvettes for optical absorption and fluorescence emission measurements. A very unusual 50-fold enhancement in the fluorescence intensity was observed in going from the 15 μM PyY aqueous solution with no CB7 to one containing 70 μM CB7 (Fig. 11). Consistent with Nau's report on the susceptibility of pyronins towards non-specific adsorption onto glass substrates [15], we were apparently not measuring photophysical effects of CB7–PyY complexation, but rather a decrease in non-specific adsorption which led to a large increase in signal. With no or little CB7 present, the low concentration of the PyY could non-specifically adsorb onto the borosilicate vials, lowering its concentration in the solutions which were transferred into quartz cuvettes for optical measurements. When the PyY samples were prepared in the presence of CB7, much less dye was apparently lost to non-specific adsorption and the increase in total dye concentration (mostly as a CB7 complex) lead to a stronger observed signal. As discussed below, PyY samples prepared in polystyrene cuvettes gave markedly different results.

The optical measurements were repeated with dilute solutions of PyY with varying amounts of CB7 prepared directly in polystyrene cuvettes. In this case, we observed only a small 1.1-fold decrease in the absorbance and modest 1.3-fold increase in fluorescence intensity for the solution containing 0.64 mM CB7 (Fig. 12). A Job's plot of PyY and CB7 indicated the formation of a 1:1 complex (Fig. S24). Full titration plots for the absorbance and fluorescence emission spectra of PyY with increasing CB7 concentration are also given in Fig. S23. A non-linear regression analysis of the fluorescence titration gave a 1:1 binding constant of $9.7 \pm 0.5 \times 10^7$ M^{-1} (Figs. S26 and S27). The binding constant for pyronin Y-CB7 was found to be 10-fold higher than for pyronin B, indicating that the *N,N*-dimethylamino groups significantly improve binding to CB7.

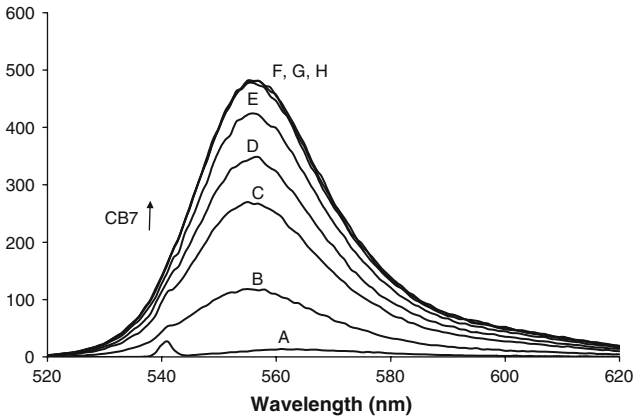

Fig. 11 Steady-state fluorescence emission spectra of aqueous pyronin Y (15 μM) at different concentrations of CB7. Samples were prepared in borosilicate glass vials and spectra were obtained using quartz cuvettes. **a** 0 μM CB7. **b** 10 μM CB7. **c** 20 μM CB7. **d** 30 μM CB7. **e** 40 μM CB7. **f** 50 μM CB7. **g** 60 μM CB7. **h** 70 μM CB7

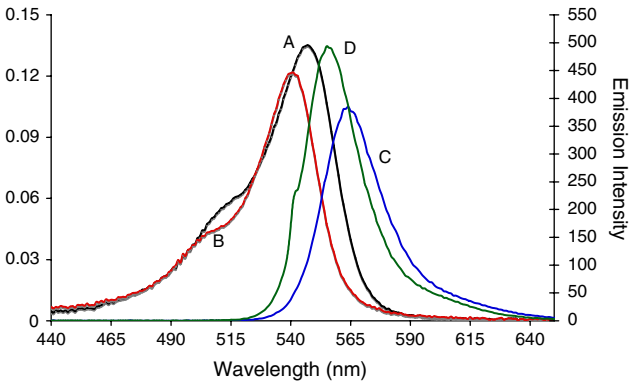

Fig. 12 UV–VIS absorption spectra (**a** at 0 mM CB7 and **b** at 0.64 mM CB7) and fluorescence emission spectra (**c** at 0 mM CB7 and **d** at 0.64 mM CB7) of aqueous pyronin Y (2.5 μM). Samples prepared and spectra obtained in polystyrene cuvettes

The NMR titration spectra are shown in Fig. S28. Unlike the PyB where strong shifts were seen for the *N,N*-diethylamino groups, the *N,N*-dimethylamino groups in PyY were not much perturbed by the addition of the CB7. A broadening and downfield shift for H-9 was seen as was a broadening and slight upfield shift for H-1/8 and H-2/7. The signal for H-4/5 broadened and did not reappear. Although it was apparent that the CB7 caused significant changes in the spectrum of PyY, firm insight into the nature of the association could not be extracted from the data.

Substrate-promoted loss of signal intensity due to non-specific adsorption of PyY onto borosilicate glass was further confirmed through a set of direct control experiments. Dilute aqueous solutions of 2.5 μM PyY with 0 mM and 0.64 mM CB7 were prepared in polystyrene cuvettes and their initial emission intensity was measured. Two samples were then transferred to a borosilicate glass vial or a polypropylene tube; the third sample was left in a polystyrene cuvette. Periodically, all three samples were transferred to fresh polystyrene cuvettes and their fluorescence emission measured before transferring back to the glass, polypropylene or polystyrene vessels. The absorbance and fluorescence emission spectra for PyY with and without 0.64 mM CB7 after 0, 1, 12 and 24 h are given for polystyrene (Fig. S29), polypropylene (Fig. S30) and borosilicate glass (Fig. S31). A summary of the data at 0 and 24 h is shown in Fig. 13. After 24 h for solutions with no CB7 present, we observed a dramatic decrease in the signal for the solution stored in borosilicate glass to just 26% of the initial signal intensity, a minor decrease in polypropylene to 95% of the original signal and essentially no change for the sample stored in polystyrene. For the samples containing 0.64 mM CB7, no changes in signal strength were found. These results confirm the statements made by Nau regarding non-specific adsorption of pyronins to borosilicate glass and the protective value of CB7 [15]. We did not, however, see the reported strong non-specific adsorption of pyronins to polypropylene.

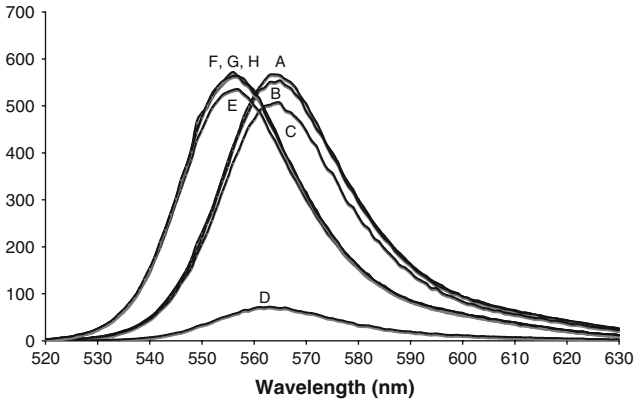

Fig. 13 Temporal evolution of the fluorescence emission intensity of aqueous pyronin Y (2.5 μM) in different sample containers with and without CB7. **a** Polystyrene, 0 h, no CB7. **b** Polystyrene, 24 h, no CB7. **c** Polypropylene, 24 h, no CB7. **d** Borosilicate glass, 24 h, no CB7. **e** Polystyrene, 0 h, 0.64 mM CB7. **f** Polystyrene, 24 h, 0.64 mM CB7. **g** Polypropylene, 24 h, 0.64 mM CB7. **h** Borosilicate glass, 24 h, 0.64 mM CB7

Conclusions

We have provided spectroscopy studies, including ^{1}H NMR, UV–Vis, and fluorescence titration experiments of cucurbit[7]uril complexes with the monocationic xanthene dyes rhodamine 6G (Rh6G, **1**), rhodamine B (RhB, **2**), rhodamine B benzyl ester (RhBBE, **3**), pyronin B (PyB, **4**) and pyronin Y (PyY, **5**). A summary of the binding constants and changes in optical properties are in Table 1. All of these cationic xanthene dyes bind strongly with cucurbit[7]uril and in all cases except for Rh6G exhibit more intense fluorescence in the presence of CB7. The binding to the linear PyB dye with its more hydrophobic *N,N*-diethyl substituents was strongest. These xanthene dyes non-specifically adsorb onto borosilicate glass but not onto polystyrene surfaces. CB7 protects against this adsorption. The data set provided here enables clearer comparisons and understanding of interactions between CB7 and these xanthene dyes; this information should be useful in the design of molecular-scale probes and photonic devices.

Table 1 Summary of association constants and changes in optical absorbance and fluorescence emission intensity of aqueous xanthene dyes with CB7

Xanthene (aqueous conc.)	K_a with CB7 (M^{-1})	Ratio of absorbance with/without CB7	Ratio of fluorescence with/without CB7
Rh6G, **1** (2.5 μM)	a	0.9 (1.0 mM CB7)	0.8 (1.0 mM CB7)
RhB, **2** (2.5 μM)	$1.6 \pm 0.4 \times 10^5$	1.3 (1.0 mM CB7)	1.6 (1.0 mM CB7)
RhBBE, **3** (2.5 μM)	$1.1 \pm 0.16 \times 10^5$	1.6 (0.64 mM CB7)	4.7 (0.64 mM CB7)
PyB, **4** (2.5 μM)	$9.1 \pm 1.6 \times 10^6$	1.0 (0.64 mM CB7)	2.3 (0.64 mM CB7)
PyY, **5** (2.5 μM)	a	0.9 (0.64 mM CB7)	1.3 (0.64 mM CB7)

[a] Values were tentative and could be fit only using CB7 concentrations less than 0.1 mM

Experimental section

Sample preparation for absorbance and fluorescence measurements

Unless otherwise noted, 1 mM aqueous solutions of each cationic dye were prepared in borosilicate glass vials using Millipore water. The 1 mM aqueous solutions were immediately diluted to the appropriate concentration in polystyrene cuvettes. For spectra obtained in quartz cuvettes, 1 mM aqueous solutions were prepared in borosilicate glass vials using Millipore water followed by subsequent dilution to the appropriate concentration in additional borosilicate glass vials. For the optical measurements, each solution was sequentially transferred to and from the quartz cuvettes.

Absorbance measurements

Absorbance measurements were performed on a UV–Vis scanning spectrophotometer. Disposable polystyrene cuvettes of 10.0 mm path were used for the measurements unless otherwise noted, in which case quartz cuvettes of 10.0 mm path were used instead. The baseline was recorded with water in both sample and reference cuvettes. All measurements were performed at ambient temperature (ca. 25 °C).

Fluorescence measurements

Steady-state measurements were performed on a spectrofluorophotometer equipped with a Xenon lamp of 150 W as the excitation source.

Disposable polystyrene cuvettes of 10.0 mm path were used for the measurements unless otherwise noted, in which case quartz cuvettes of 10.0 mm path were used instead. The slit width was adjusted to the minimum setting for all measurements. Measurements were performed at ambient temperature. A 0.5 neutral density filter was used for all measurements except those obtained for aqueous solutions of Pyronin Y at 2.5 μM, in which case no filter was required. Although duplicate measurements were made, single point data from selected single measurements were plotted and used for the binding analyses.

Rhodamine B benzyl ester (3)

A mixture of rhodamine B (1.0 g, 2.0 mmol), methylene chloride (40 mL), 1,3-dicyclohexyl carbodiimide (0.474 g, 2.3 mmol), benzyl alcohol (0.249 g, 2.3 mmol), and 4-(*N,N*-dimethylamino)pyridine (0.026 g, 0.2 mmol) was stirred under nitrogen at room temperature for 19 h. The crude dark pink filtrate was collected via vacuum filtration and concentrated at room temperature under reduced pressure. A portion of the crude product (0.106 g) was purified via silica gel column chromatography (methanol/chloroform, 9:1), (methanol/chloroform/glacial acetic acid, 90:10:1), respectively, to give 0.056 g (0.10 mmol, 53%) of pure **3** as a purple/red waxy solid: ^{1}H NMR (300 MHz, CD_3CN): δ 8.29 (m, 1H), 7.80 (m, 2H), 7.34 (m, 1H), 7.21 (m, 3H), 7.01 (d, $J = 9.5$ Hz, 2H), 6.87 (dd, $J = 2.5$, 9.5 Hz, 4H), 6.67 (d, $J = 2.5$ Hz, 2H), 4.90 (s, 2H), 3.61 (q, $J = 7.1$ Hz, 8H), 1.26 (t, $J = 7.1$ Hz, 12H). ^{13}C NMR (75 MHz, CD_3CN): δ 173.7, 165.3, 158.1, 157.6, 155.6, 134.8, 133.3, 132.9, 131.2, 131.1, 130.3, 130.2, 130.1, 128.5, 128.3, 128.1, 114.2, 113.4, 95.9, 67.3, 45.6, 11.9. MS (ESI): *m/z* 533.33 $[M\text{-}Cl]^+$ (100%), 443.27 (5%), ($M = C_{35}H_{37}N_2O_3^+$ requires 533.28).

Acknowledgements Support through NSF (DMR-0805233) and from the University of Oklahoma and Oklahoma State Regents for Higher Education is appreciated. JLM acknowledges the DOEd for a GAANN Fellowship. KY, JAIH, KAW acknowledge support through the Undergraduate Research Program.

References

1. Aslan, K., Gryczynski, I., Malicka, J., Matveeva, E., Lakowicz, J.R., Geddes, C.D.: Metal-enhanced fluorescence: an emerging tool in biotechnology. Curr. Opin. Biotechnol. **16**, 55–62 (2005)
2. Dooley, C.T., Dore, T.M., Hansom, G.T., Jackson, W.C., Remington, S.J., Tsien, R.Y.: Imaging dynamic redox changes in mammalian cells with green fluorescent protein indicators. J. Biol. Chem. **279**, 22284–22293 (2004)
3. Kettling, U., Koltermann, A., Schwille, P., Eigen, M.: Real-time enzyme kinetics monitored by dual-color fluorescence cross-correlation spectroscopy. Proc. Natl. Acad. Sci. USA. **95**, 1416–1420 (1998)
4. Yan, P., Holman, M.W., Robustelli, P., Chowdhury, A., Ishak, F.I., Adams, D.M.: Molecular switch based on a biologically important redox reaction. J. Phys. Chem. B **109**, 130–137 (2005)
5. Zhang, Y.B., Kanungo, M., Ho, A.J., Freimuth, P., van der Lelie, D., Chen, M., Khamis, S.M., Datta, S.S., Johnson, A.T.C., Misewich, J.A., Wong, S.S.: Functionalized carbon nanotubes for detecting viral proteins. Nano Lett. **7**, 3086–3091 (2007)
6. Palacios, R.E., Fan, F.-R.F., Bard, A.J., Barbara, P.F.: Single-molecule spectroelectrochemistry (SMS-EC). J. Am. Chem. Soc. **128**, 9028–9029 (2006)
7. Fabbrizzi, L., Poggi, A.: Sensors and switches from supramolecular chemistry. Chem. Soc. Rev. **25**, 197–202 (1995)
8. Arunkumar, E., Forbes, C.C., Smith, B.D.: Improving the properties of organic dyes by molecular encapsulation. Eur. J. Org. Chem. **2005**, 4051–4059 (2005)
9. Mohanty, J., Bhasikuttan, A.C., Nau, W.M., Pal, H.: Host-guest complexation of neutral red with macrocyclic host molecules: contrasting pK(sub a) shifts and binding affinities for cucurbit[7]uril and b-cyclodextrin. J. Phys. Chem. B **110**, 5132–5138 (2006)
10. Rohatgi, K.K., Singhal, G.S.: Nature of bonding in dye aggregates. J. Phys. Chem. **70**, 1695–1701 (1966)
11. Selwyn, J.E., Steinfeld, J.I.: Aggregation equilibria of xanthene dyes. J. Phys. Chem. **76**, 762–774 (1972)

12. Vosch, T., Hofkens, J., Cotlet, M., Köhn, F., Fujiwara, H., Gronheid, R., van der Biest, K., Weil, T., Herrmann, A., Müllen, K., Mukamel, S., van der Auweraer, M., de Schryver, F.C.: Influence of structural and rotational isomerism on the triplet blinking of individual dendrimer molecules. Angew. Chem. Int. Ed **40**, 4643–4648 (2001)
13. Tinnefeld, P., Buschmann, V., Weston, K.D., Sauer, M.: Direct observation of collective blinking and energy transfer in a bichromophoric system. J. Phys. Chem. A **107**, 323–327 (2003)
14. Lee, T.-H., Gonzalez, J.I., Zheng, J., Dickson, R.M.: Single molecule optoelectronics. Acc. Chem. Res. **38**, 534–541 (2005)
15. Nau, W.M., Mohanty, J.: Taming fluorescent dyes with cucurbit[7]uril. Inter. J. Photoenergy **7**, 717–726 (2005)
16. Mohanty, J., Nau, W.M.: Ultrastable rhodamine with cucurbituril. Angew. Chem. Int. Ed **44**, 3750–3754 (2005)
17. Buschmann, H.-J., Schollmeyer, E.: Stabilization of dyes against hydrolytic decomposition by the formation of inclusion compounds. J. Incl. Phenom. Macro. Chem. **7**, 133–141 (1992)
18. Freeman, W.A., Mock, W.L., Shih, N.Y.: Cucurbituril. J. Am. Chem. Soc. **103**, 7367–7368 (1981)
19. Day, A., Arnold, A.P., Blanch, R.J., Snushall, B.: Controlling factors in the synthesis of cucurbituril and its homologues. J. Org. Chem. **66**, 8094–8100 (2001)
20. Kim, J., Jung, I., Kim, S., Lee, E., Kang, J., Sakamoto, S., Yamaguchi, K., Kim, K.: New cucurbituril homologues: synthesis, isolation characterization and X-ray crystal structures of cucurbit[n]uril ($n = 5$, 7 and 8). J. Am. Chem. Soc. **122**, 540–541 (2000)
21. Lagona, J., Mukhopadhyay, P., Chakrabarti, S., Isaacs, L.: The cucurbit[n]uril family. Angew. Chem. Int. Ed **44**, 4844–4870 (2005)
22. Saleh, N., Al-Rawashdeh, N.A.F.: Fluorescence enhancement of cabendazim fungicide in cucurbit[6]uril. J. Fluoresc. **16**, 487–493 (2006)
23. Maafi, M., Laassis, B., Aaron, J.-J.: Photochemically induced fluorescence investigation of b-cyclodextrin; azure A inclusion complex and determination of analytical parameters. J. Incl. Phenom. Macro. Chem. **22**, 235–247 (1995)
24. Singh, M.K., Pal, H., Koti, A.S.R., Sapre, A.V.: Photophysical properties and rotational relaxation dynamics of neutral red bound to b-cyclodextrin. J. Phys. Chem. A **108**, 1465–1474 (2004)
25. Schiller, R.L., Lincoln, S.F., Coates, J.H.: The inclusion of pyronine Y by b- and g-cyclodextrin. J. Chem. Soc. Faraday Trans. **83**, 3237–3248 (1987)
26. Reija, B., Al-Soufi, W., Novo, M., Tato, J.V.: Specific interactions in the inclusion complexes of pyronines Y and B with b-cyclodextrin. J. Phys. Chem. B **109**, 1364–1370 (2005)
27. Wang, R., Yuan, L., Macartney, D.H.: A green to blue fluorescence switch of protonated 2-aminoanthracene upon inclusion in cucurbit[7]uril. Chem. Commun. 5867–5869 (2005)
28. Wagner, B.D., Stojanovic, N., Day, A.I., Blanch, R.J.: Host properties of cucurbit[7]uril: fluorescence enhancement of anilinonaphthalene sulfonates. J. Phys. Chem. B **107**, 10741–10746 (2003)
29. Mohanty, J., Pal, H., Ray, A.K., Kumar, S., Nau, W.M.: Supramolecular dye laser with cucurbit[7]uril in water. Chem. Phys. Chem. **8**, 54–56 (2007)
30. Martyn, T.A., Moore, J.L., Halterman, R.L., Yip, W.T.: Cucurbit[7]uril induces superior probe performance for single-molecule detection. J. Am. Chem. Soc. **129**, 10338–10339 (2007)
31. Halterman, R.L., Moore, J.L., Mannel, L.M.: Disrupting aggregation of tethered rhodamine B dyads through inclusion in cucurbit[7]uril. J. Org. Chem. **73**, 3266–3269 (2008)
32. Ingham, K.C.: On the application of job's method of continuous variation to the stoichiometry of protein-ligand complexes. Anal. Biochem. **68**, 660–663 (1975)
33. Likussar, W., Boltz, D.F.: Theory of continuous variations plots and a new method for spectrophotometric determination of extraction and formation constants. Anal. Chem. **43**, 1265–1271 (1971)
34. Ong, W., Gomez-Kaifer, M., Kaifer, A.E.: Cucurbit[7]uril: a very effective host for viologens and their cation radicals. Org. Lett. **4**, 1791–1794 (2002)
35. Gutierrez, M.C., Hortiguela, M.J., Ferrer, M.L., delMonte, F.: Highly fluorescent rhodamine B nanoparticles entrapped in hybrid glasses. Langmuir **23**, 2175–2179 (2007)
36. Klika, Z., Weissmannova, H., Capkova, P., Pospisil, M.: The rhodamine B intercalation of montmorillonite. J. Coll. Interface Sci. **275**, 243–250 (2004)
37. Hassner, A., Alexanian, V.: Direct room temperature esterification of carboxylic acids. Tetrahedron Lett. **46**, 4475–4478 (1978)